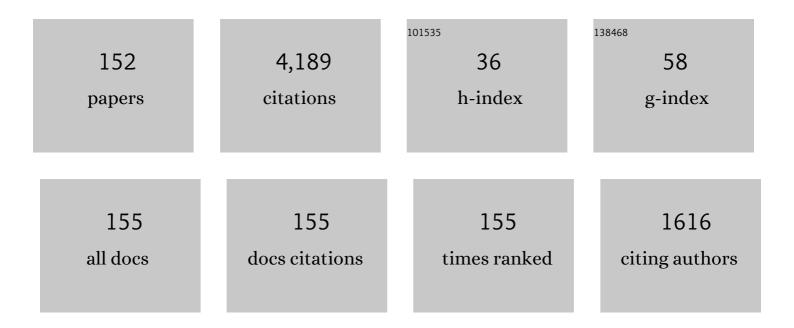
Keith A Wear

List of Publications by Year in descending order

Source: https://exaly.com/author-pdf/7333064/publications.pdf Version: 2024-02-01



Κειτή Δ \λ/ελ

#	Article	IF	CITATIONS
1	Tissue-mimicking phantoms for performance evaluation of photoacoustic microscopy systems. Biomedical Optics Express, 2022, 13, 1357.	2.9	1
2	Spatiotemporal Deconvolution of Hydrophone Response for Linear and Nonlinear Beams—Part I: Theory, Spatial-Averaging Correction Formulas, and Criteria for Sensitive Element Size. IEEE Transactions on Ultrasonics, Ferroelectrics, and Frequency Control, 2022, 69, 1243-1256.	3.0	8
3	Spatiotemporal Deconvolution of Hydrophone Response for Linear and Nonlinear Beams—Part II: Experimental Validation. IEEE Transactions on Ultrasonics, Ferroelectrics, and Frequency Control, 2022, 69, 1257-1267.	3.0	6
4	Photoacoustic imaging phantoms for assessment of object detectability and boundary buildup artifacts. Photoacoustics, 2022, 26, 100348.	7.8	6
5	Scattering in Cancellous Bone. Advances in Experimental Medicine and Biology, 2022, 1364, 163-175.	1.6	1
6	Biomechanical structure–function relations for human trabecular bone — comparison of calcaneus, femoral neck, greater trochanter, proximal tibia, and vertebra. Computer Methods in Biomechanics and Biomedical Engineering, 2022, , 1-9.	1.6	0
7	Radiological Society of North America/Quantitative Imaging Biomarker Alliance Shear Wave Speed Bias Quantification in Elastic and Viscoelastic Phantoms. Journal of Ultrasound in Medicine, 2021, 40, 569-581.	1.7	25
8	Hydrophone Spatial Averaging Correction for Acoustic Exposure Measurements From Arrays—Part II: Validation for ARFI and Pulsed Doppler Waveforms. IEEE Transactions on Ultrasonics, Ferroelectrics, and Frequency Control, 2021, 68, 376-388.	3.0	15
9	Note to Physicians and Sonographers on Potential Underestimation of Acoustic Safety Indexes for Diagnostic Array Transducers. IEEE Transactions on Ultrasonics, Ferroelectrics, and Frequency Control, 2021, 68, 357-357.	3.0	7
10	Hydrophone Spatial Averaging Correction for Acoustic Exposure Measurements From Arrays—Part I: Theory and Impact on Diagnostic Safety Indexes. IEEE Transactions on Ultrasonics, Ferroelectrics, and Frequency Control, 2021, 68, 358-375.	3.0	16
11	Polyacrylamide hydrogel phantoms for performance evaluation of multispectral photoacoustic imaging systems. Photoacoustics, 2021, 22, 100245.	7.8	17
12	AAPM Task Group 241: A medical physicist's guide to MRIâ€guided focused ultrasound body systems. Medical Physics, 2021, 48, e772-e806.	3.0	9
13	Mechanisms of Interaction of Ultrasound With Cancellous Bone: A Review. IEEE Transactions on Ultrasonics, Ferroelectrics, and Frequency Control, 2020, 67, 454-482.	3.0	55
14	Correction for Hydrophone Spatial Averaging Artifacts for Circular Sources. IEEE Transactions on Ultrasonics, Ferroelectrics, and Frequency Control, 2020, 67, 2674-2691.	3.0	12
15	Evaluation of Fluence Correction Algorithms in Multispectral Photoacoustic Imaging. Photoacoustics, 2020, 19, 100181.	7.8	20
16	Hydrophone Spatial Averaging Artifacts for Pulsed Doppler Beams from Array Transducers. , 2020, , .		1
17	Hydrophone Spatial Averaging Artifacts for ARFI Beams from Array Transducers. , 2020, , .		1
18	Correction for Spatial Averaging Artifacts for Circularly-Symmetric Pressure Beams Measured with		1

Membrane Hydrophones. , 2020, , .

#	Article	IF	CITATIONS
19	Correction for Spatial Averaging Artifacts in Hydrophone Measurements of High-Intensity Therapeutic Ultrasound: An Inverse Filter Approach. IEEE Transactions on Ultrasonics, Ferroelectrics, and Frequency Control, 2019, 66, 1453-1464.	3.0	20
20	Directivity and Frequency-Dependent Effective Sensitive Element Size of Membrane Hydrophones: Theory Versus Experiment. IEEE Transactions on Ultrasonics, Ferroelectrics, and Frequency Control, 2019, 66, 1723-1730.	3.0	20
21	Considerations for Choosing Sensitive Element Size for Needle and Fiber-Optic Hydrophones—Part I: Spatiotemporal Transfer Function and Graphical Guide. IEEE Transactions on Ultrasonics, Ferroelectrics, and Frequency Control, 2019, 66, 318-339.	3.0	23
22	Considerations for Choosing Sensitive Element Size for Needle and Fiber-Optic Hydrophones—Part II: Experimental Validation of Spatial Averaging Model. IEEE Transactions on Ultrasonics, Ferroelectrics, and Frequency Control, 2019, 66, 340-347.	3.0	20
23	Multidomain computational modeling of photoacoustic imaging: verification, validation, and image quality prediction. Journal of Biomedical Optics, 2019, 24, 1.	2.6	7
24	Experimental investigation of parameters influencing plasmonic nanoparticle-mediated bubble generation with nanosecond laser pulses. Journal of Biomedical Optics, 2019, 24, 1.	2.6	17
25	Photoacoustic oximetry imaging performance evaluation using dynamic blood flow phantoms with tunable oxygen saturation. Biomedical Optics Express, 2019, 10, 449.	2.9	35
26	Pulsed laser damage of gold nanorods in turbid media and its impact on multi-spectral photoacoustic imaging. Biomedical Optics Express, 2019, 10, 1919.	2.9	10
27	Pressure Pulse Distortion by Needle and Fiber-Optic Hydrophones due to Nonuniform Sensitivity. IEEE Transactions on Ultrasonics, Ferroelectrics, and Frequency Control, 2018, 65, 137-148.	3.0	18
28	Directivity and Frequency-Dependent Effective Sensitive Element Size of a Reflectance-Based Fiber-Optic Hydrophone: Predictions From Theoretical Models Compared With Measurements. IEEE Transactions on Ultrasonics, Ferroelectrics, and Frequency Control, 2018, 65, 2343-2348.	3.0	26
29	Directivity and Frequency-Dependent Effective Sensitive Element Size of Needle Hydrophones: Predictions From Four Theoretical Forms Compared With Measurements. IEEE Transactions on Ultrasonics, Ferroelectrics, and Frequency Control, 2018, 65, 1781-1788.	3.0	32
30	Broadband characterization of plastic and high intensity therapeutic ultrasound phantoms using time delay spectrometry—With validation using Kramers–Kronig relations. Journal of the Acoustical Society of America, 2018, 143, 3365-3372.	1.1	5
31	Size-dependent thresholds for melting and nanobubble generation using pulsed-laser irradiated gold nanoparticles. , 2018, , .		4
32	Performance evaluation of photoacoustic oximetry imaging systems using a dynamic blood flow phantom with tunable oxygen saturation. , 2018, , .		2
33	Pulsed-Laser-Induced Modification of Gold Nanorods: Damage Thresholds and Impact on Photoacoustic Imaging in Turbid Media. , 2018, , .		0
34	Evaluation of Oximetry Measurement Accuracy of Multispectral Photoacoustic Imaging Systems Using a Dynamically Tunable Blood Flow Phantom. , 2018, , .		0
35	Development and validation of a biologically realistic tissue-mimicking material for photoacoustics and other bimodal optical-acoustic modalities. Proceedings of SPIE, 2017, , .	0.8	1
36	Variation of High-Intensity Therapeutic Ultrasound (HITU) Pressure Field Characterization: Effects of Hydrophone Choice, Nonlinearity, Spatial Averaging and Complex Deconvolution. Ultrasound in Medicine and Biology, 2017, 43, 2329-2342.	1.5	32

#	Article	IF	CITATIONS
37	Relationships among ultrasonic and mechanical properties of cancellous bone in human calcaneus in vitro. Bone, 2017, 103, 93-101.	2.9	28
38	Notice of Removal: Regulation of medical ultrasound devices in the United States of America. , 2017, , .		0
39	Two-layer heterogeneous breast phantom for photoacoustic imaging. Journal of Biomedical Optics, 2017, 22, 1.	2.6	17
40	Phantom-based image quality test methods for photoacoustic imaging systems. Journal of Biomedical Optics, 2017, 22, 1.	2.6	20
41	Evaluation of Out-of-Plane Sensitivity and Artifacts in Photoacoustic Imaging. , 2017, , .		0
42	A suite of phantom-based test methods for assessing image quality of photoacoustic tomography systems. Proceedings of SPIE, 2017, , .	0.8	0
43	Nanoparticle-enhanced spectral photoacoustic tomography: effect of oxygen saturation and tissue heterogeneity. , 2016, , .		0
44	Biologically relevant photoacoustic imaging phantoms with tunable optical and acoustic properties. Journal of Biomedical Optics, 2016, 21, 101405.	2.6	85
45	Conventional, Bayesian, and Modified Prony's methods for characterizing fast and slow waves in equine cancellous bone. Journal of the Acoustical Society of America, 2015, 138, 594-604.	1.1	8
46	RSNA QIBA ultrasound shear wave speed Phase II phantom study in viscoelastic media. , 2015, , .		33
47	Design and phantom-based validation of a bimodal ultrasound-photoacoustic imaging system for spectral detection of optical biomarkers. , 2015, , .		3
48	Quantitative assessment of photoacoustic tomography systems integrating clinical ultrasound transducers using novel tissue-simulating phantoms. Proceedings of SPIE, 2015, , .	0.8	6
49	Correction for frequency-dependent hydrophone response to nonlinear pressure waves using complex deconvolution and rarefactional filtering: application with fiber optic hydrophones. IEEE Transactions on Ultrasonics, Ferroelectrics, and Frequency Control, 2015, 62, 152-164.	3.0	37
50	Conditionally Increased Acoustic Pressures in Nonfetal Diagnostic Ultrasound Examinations Without Contrast Agents: A Preliminary Assessment. Journal of Ultrasound in Medicine, 2015, 34, 1-41.	1.7	48
51	Nonlinear attenuation and dispersion in human calcaneusin vitro: Statistical validation and relationships to microarchitecture. Journal of the Acoustical Society of America, 2015, 137, 1126-1133.	1.1	5
52	Lesion detectability in automated breast ultrasound. Proceedings of SPIE, 2014, , .	0.8	0
53	Fast and slow wave detection in bovine cancellous bone in vitro using bandlimited deconvolution and Prony's method. Journal of the Acoustical Society of America, 2014, 136, 2015-2024.	1.1	13
54	Temporal evolution of fast and slow waves during propagation through bovine cancellous bone in vitro. , 2014, , .		0

#	Article	IF	CITATIONS
55	Suppression of pressure measurement artifacts from fiber optic hydrophones using complex deconvolution of sensitivity. , 2014, , .		0
56	Time-domain separation of interfering waves in cancellous bone using bandlimited deconvolution: Simulation and phantom study. Journal of the Acoustical Society of America, 2014, 135, 2102-2112.	1.1	16
57	Improved measurement of acoustic output using complex deconvolution of hydrophone sensitivity. IEEE Transactions on Ultrasonics, Ferroelectrics, and Frequency Control, 2014, 61, 62-75.	3.0	59
58	Estimation of fast and slow wave properties in cancellous bone using Prony's method and curve fitting. Journal of the Acoustical Society of America, 2013, 133, 2490-2501.	1.1	13
59	RSNA/QIBA: Shear wave speed as a biomarker for liver fibrosis staging. , 2013, , .		52
60	Relationships of quantitative ultrasound parameters with cancellous bone microstructure in human calcaneus in vitro. Journal of the Acoustical Society of America, 2012, 131, 1605-1612.	1.1	65
61	Phase measurement with a simplified ultrasonic time delay spectrometry system. , 2012, , .		1
62	Comparison of hydrophone phase response obtained via time delay spectrometry measurement and Hilbert transformation. AIP Conference Proceedings, 2012, , .	0.4	2
63	Development and characterization of a tissue-mimicking material for high-intensity focused ultrasound. IEEE Transactions on Ultrasonics, Ferroelectrics, and Frequency Control, 2011, 58, 1397-1405.	3.0	53
64	Time-delay spectrometry measurement of magnitude and phase of hydrophone response. IEEE Transactions on Ultrasonics, Ferroelectrics, and Frequency Control, 2011, 58, 2325-2333.	3.0	35
65	Scattering by Trabecular Bone. , 2011, , 123-145.		9
66	Decomposition of Two-Component Ultrasound Pulses in Cancellous Bone Using Modified Least Squares Prony Method – Phantom Experiment and Simulation. Ultrasound in Medicine and Biology, 2010, 36, 276-287.	1.5	32
67	Robert F. Wagner 1938–2008. Ultrasonic Imaging, 2010, 32, 129-130.	2.6	0
68	Cancellous bone analysis with modified least squares Prony's method and chirp filter: Phantom experiments and simulation. Journal of the Acoustical Society of America, 2010, 128, 2191-2203.	1.1	29
69	Decomposition of two-component pulses in bone: Phantom experiment and simulation. , 2010, , .		0
70	The dependencies of phase velocity and dispersion on volume fraction in cancellous-bone-mimicking phantoms. Journal of the Acoustical Society of America, 2009, 125, 1197-1201.	1.1	21
71	Frequency dependence of average phase shift from human calcaneus in vitro. Journal of the Acoustical Society of America, 2009, 126, 3291-3300.	1.1	7
72	Temperature-dependent Physical Properties of a HIFU Blood Mimicking Fluid. AIP Conference Proceedings, 2009, , .	0.4	1

#	Article	IF	CITATIONS
73	Measurements of Ultrasonic Backscattered Spectral Centroid Shift From Spine In Vivo: Methodology and Preliminary Results. Ultrasound in Medicine and Biology, 2009, 35, 165-168.	1.5	39
74	A method for improved standardization of in vivo calcaneal time-domain speed-of-sound measurements. IEEE Transactions on Ultrasonics, Ferroelectrics, and Frequency Control, 2008, 55, 1473-1479.	3.0	10
75	Mechanisms for attenuation in cancellous-bone-mimicking phantoms. IEEE Transactions on Ultrasonics, Ferroelectrics, and Frequency Control, 2008, 55, 2418-2425.	3.0	26
76	Frequency dependence of backscatter from thin, oblique, finite-length cylinders measured with a focused transducer - with applications in cancellous bone. , 2008, , .		0
77	Ultrasonic scattering from cancellous bone: A review. IEEE Transactions on Ultrasonics, Ferroelectrics, and Frequency Control, 2008, 55, 1432-1441.	3.0	108
78	The effect of phase cancellation on estimates of broadband ultrasound attenuation and backscatter coefficient in human calcaneus in vitro. IEEE Transactions on Ultrasonics, Ferroelectrics, and Frequency Control, 2008, 55, 384-390.	3.0	23
79	Interference between wave modes may contribute to the apparent negative dispersion observed in cancellous bone. Journal of the Acoustical Society of America, 2008, 124, 1781-1789.	1.1	59
80	Introduction to the special issue on diagnostic and therapeutic applications of ultrasound in bone - Part I. IEEE Transactions on Ultrasonics, Ferroelectrics, and Frequency Control, 2008, 55, 1177-1178.	3.0	5
81	Comparison of the Faran Cylinder Model and the Weak Scattering Model for predicting the frequency dependence of backscatter from human cancellous femur in vitro. Journal of the Acoustical Society of America, 2008, 124, 1408-1410.	1.1	9
82	Frequency dependence of backscatter from thin, oblique, finite-length cylinders measured with a focused transducer-with applications in cancellous bone. Journal of the Acoustical Society of America, 2008, 124, 3309-3314.	1.1	16
83	Ultrasonic attenuation in parallel-nylon-wire cancellous-bone-mimicking phantoms. Journal of the Acoustical Society of America, 2008, 124, 4042-4046.	1.1	9
84	Development and characterization of a blood mimicking fluid for high intensity focused ultrasound. Journal of the Acoustical Society of America, 2008, 124, 1803-1810.	1.1	12
85	Introduction to the special issue on diagnostic and therapeutic applications of ultrasound in bone-part II. IEEE Transactions on Ultrasonics, Ferroelectrics, and Frequency Control, 2008, 55, 1415-1416.	3.0	3
86	P5A-1 A Method for Improved Standardization of In Vivo Calcaneal Time-Domain Speed-of-Sound Measurements. Proceedings IEEE Ultrasonics Symposium, 2007, , .	0.0	0
87	PARAMETER ESTIMATION IN ULTRASONIC MEASUREMENTS ON TRABECULAR BONE. AIP Conference Proceedings, 2007, , .	0.4	4
88	The dependence of time-domain speed-of-sound measurements on center frequency, bandwidth, and transit-time marker in human calcaneus <i>in vitro</i> . Journal of the Acoustical Society of America, 2007, 122, 636-644.	1.1	13
89	Model Selection in Ultrasonic Measurements on Trabecular Bone. AIP Conference Proceedings, 2007, ,	0.4	3
90	12C-2 Improved Accuracy of Broadband Ultrasound Attenuation Measurement Using Phase Insensitive Detection: Results in 73 Women. Proceedings IEEE Ultrasonics Symposium, 2007, , .	0.0	0

#	Article	IF	CITATIONS
91	Development of a HIFU Phantom. AIP Conference Proceedings, 2007, , .	0.4	22
92	Group velocity, phase velocity, and dispersion in human calcaneus in vivo. Journal of the Acoustical Society of America, 2007, 121, 2431-2437.	1.1	41
93	The Effect of Phase Cancellation on Estimates of Calcaneal Broadband Ultrasound Attenuation in Vivo. IEEE Transactions on Ultrasonics, Ferroelectrics, and Frequency Control, 2007, 54, 1352-1359.	3.0	29
94	Fred Lizzi's Statistical Framework and the Interpretation of Ultrasound Backscatter from Bone. Ultrasonic Imaging, 2006, 28, 41-42.	2.6	4
95	Interlaboratory Comparison of Ultrasonic Backscatter Coefficient Measurements From 2 to 9 MHz. Journal of Ultrasound in Medicine, 2005, 24, 1235-1250.	1.7	135
96	The dependencies of phase velocity and dispersion on trabecular thickness and spacing in trabecular bone-mimicking phantoms. Journal of the Acoustical Society of America, 2005, 118, 1186-1192.	1.1	50
97	Comparison of measurements of phase velocity in human calcaneus to Biot theory. Journal of the Acoustical Society of America, 2005, 117, 3319-3324.	1.1	54
98	Measurement of dependence of backscatter coefficient from cylinders on frequency and diameter using focused transducers—with applications in trabecular bone. Journal of the Acoustical Society of America, 2004, 115, 66-72.	1.1	36
99	The dependence of ultrasonic backscatter on trabecular thickness in human calcaneus: theoretical and experimental results. IEEE Transactions on Ultrasonics, Ferroelectrics, and Frequency Control, 2003, 50, 979-986.	3.0	48
100	Characterization of trabecular bone using the backscattered spectral centroid shift. IEEE Transactions on Ultrasonics, Ferroelectrics, and Frequency Control, 2003, 50, 402-407.	3.0	43
101	Autocorrelation and cepstral methods for measurement of tibial cortical thickness. IEEE Transactions on Ultrasonics, Ferroelectrics, and Frequency Control, 2003, 50, 655-660.	3.0	40
102	The effect of trabecular material properties on the frequency dependence of backscatter from cancellous bone (L). Journal of the Acoustical Society of America, 2003, 114, 62-65.	1.1	18
103	Measurements of ultrasonic backscattered spectral centroid shift from spine in vivo: methodology and preliminary results. , 2003, , .		1
104	Relationship between ultrasonic backscatter and trabecular thickness in human calcaneus: theory and experiment. , 2003, 5035, 109.		0
105	A Gaussian framework for modeling effects of frequency-dependent attenuation, frequency-dependent scattering, and gating. IEEE Transactions on Ultrasonics, Ferroelectrics, and Frequency Control, 2002, 49, 1572-1582.	3.0	22
106	A stratified model to predict dispersion in trabecular bone. IEEE Transactions on Ultrasonics, Ferroelectrics, and Frequency Control, 2001, 48, 1079-1083.	3.0	62
107	<title>Computer simulation and experiments to investigate the effects of frequency-dependent
attenuation and dispersion on speed-of-sound estimates in cancellous bone</title> . , 2001, 4325, 356.		0
108	<title>Fundamental mechanisms underlying broadband ultrasonic attenuation in calcaneus</title> . , 2001, , .		0

#	Article	IF	CITATIONS
109	Ultrasonic attenuation in human calcaneus from 0.2 to 1.7 MHz. IEEE Transactions on Ultrasonics, Ferroelectrics, and Frequency Control, 2001, 48, 602-608.	3.0	71
110	Relationships among calcaneal backscatter, attenuation, sound speed, hip bone mineral density, and age in normal adult women. Journal of the Acoustical Society of America, 2001, 110, 573-578.	1.1	36
111	A numerical method to predict the effects of frequency-dependent attenuation and dispersion on speed of sound estimates in cancellous bone. Journal of the Acoustical Society of America, 2001, 109, 1213-1218.	1.1	25
112	Fundamental precision limitations for measurements of frequency dependence of backscatter: Applications in tissue-mimicking phantoms and trabecular bone. Journal of the Acoustical Society of America, 2001, 110, 3275-3282.	1.1	37
113	Relationships of ultrasonic backscatter with ultrasonic attenuation, sound speed and bone mineral density in human calcaneus. Ultrasound in Medicine and Biology, 2000, 26, 1311-1316.	1.5	63
114	Candidate mechanisms to explain temperature dependence of ultrasonic attenuation in human calcaneus. Ultrasound in Medicine and Biology, 2000, 26, 1370.	1.5	1
115	Temperature dependence of ultrasonic attenuation in human calcaneus. Ultrasound in Medicine and Biology, 2000, 26, 469-472.	1.5	20
116	Measurements of phase velocity and group velocity in human calcaneus. Ultrasound in Medicine and Biology, 2000, 26, 641-646.	1.5	118
117	<title>Variations in transit-time-based ultrasonic velocity estimates in human calcaneus due to frequency-dependent attenuation and dispersion</title> . , 2000, 3982, 187.		0
118	Anisotropy of ultrasonic backscatter and attenuation from human calcaneus: Implications for relative roles of absorption and scattering in determining attenuation. Journal of the Acoustical Society of America, 2000, 107, 3474-3479.	1,1	79
119	The effects of frequency-dependent attenuation and dispersion on sound speed measurements: applications in human trabecular bone. IEEE Transactions on Ultrasonics, Ferroelectrics, and Frequency Control, 2000, 47, 265-273.	3.0	108
120	The relationship between ultrasonic backscatter and bone mineral density in human calcaneus. IEEE Transactions on Ultrasonics, Ferroelectrics, and Frequency Control, 2000, 47, 777-780.	3.0	29
121	Frequency dependence of ultrasonic backscatter from human trabecular bone: Theory and experiment. Journal of the Acoustical Society of America, 1999, 106, 3659-3664.	1.1	173
122	Uncertainties in estimates of lesion detectability in diagnostic ultrasound. Journal of the Acoustical Society of America, 1999, 106, 1161-1173.	1.1	5
123	<title>Using phase information to characterize coherent scattering from regular structures in ultrasound signals</title> . , 1999, 3661, 654.		1
124	Interlaboratory comparison of ultrasonic backscatter, attenuation, and speed measurements Journal of Ultrasound in Medicine, 1999, 18, 615-631.	1.7	172
125	Assessment of bone density using ultrasonic backscatter. Ultrasound in Medicine and Biology, 1998, 24, 689-695.	1.5	105
126	<title>Quantitative ultrasound tissue characterization using texture and cepstral features</title> . , 1998, , .		1

#	Article	IF	CITATIONS
127	Statistical properties of estimates of signal-to-noise ratio and number of scatterers per resolution cell. Journal of the Acoustical Society of America, 1997, 102, 635-641.	1.1	20
128	Constrained reconstruction applied to 2-D chemical shift imaging. IEEE Transactions on Medical Imaging, 1997, 16, 591-597.	8.9	9
129	<title>Mean scatterer-spacing estimation using the complex cepstrum</title> . , 1997, , .		1
130	Quantitative estimation of scatterer spacing from backscattered ultrasound signals using the complex cepstrum. Lecture Notes in Computer Science, 1997, , 513-518.	1.3	8
131	Measurements of ultrasonic backscatter coefficients in human liver and kidney in vivo. Journal of the Acoustical Society of America, 1995, 98, 1852-1857.	1.1	52
132	Quantitative assessment of myocardial ultrasound tissue characterization through receiver operating characteristic analysis of Bayesian classifiers. Journal of the American College of Cardiology, 1995, 25, 1706-1711.	2.8	33
133	A comparison of autoregressive spectral estimation algorithms and order determination methods in ultrasonic tissue characterization. IEEE Transactions on Ultrasonics, Ferroelectrics, and Frequency Control, 1995, 42, 709-716.	3.0	40
134	An Autoregressive Method for High-Resolution One-Dimensional Chemical-Shift Imaging. Journal of Magnetic Resonance Series B, 1994, 105, 172-176.	1.6	3
135	High resolution ultrasonic backscatter coefficient estimation based on autoregressive spectral estimation using Burg's algorithm. IEEE Transactions on Medical Imaging, 1994, 13, 500-507.	8.9	35
136	<title>Combining a few diagnostic tests or features</title> . , 1994, 2167, 503.		4
137	Application of autoregressive spectral analysis to cepstral estimation of mean scatterer spacing. IEEE Transactions on Ultrasonics, Ferroelectrics, and Frequency Control, 1993, 40, 50-58.	3.0	136
138	<title>Comparison of methods for spectral estimation from 1D NMR time signals</title> . , 1992, , .		0
139	The effect of frequency on the magnitude of cyclic variation of backscatter in dogs and implications for prompt detection of acute myocardial ischemia. IEEE Transactions on Ultrasonics, Ferroelectrics, and Frequency Control, 1991, 38, 498-502.	3.0	12
140	Application of parametric spectral estimation to medical ultrasound and magnetic resonance spectroscopy. , 1990, 1231, 34.		3
141	Myocardial ultrasonic backscatter for characterization of ischemia and reperfusion: relationship to wall motion. Ultrasound in Medicine and Biology, 1990, 16, 391-398.	1.5	36
142	Ultrasonic tissue characterization with integrated backscatter. Acute myocardial ischemia, reperfusion, and stunned myocardium in patients Circulation, 1989, 80, 491-503.	1.6	195
143	Differentiation between acutely ischemic myocardium and zones of completed infarction in dogs on the basis of frequencyâ€dependent backscatter. Journal of the Acoustical Society of America, 1989, 85, 2634-2641.	1.1	55
144	Contractionâ€related variation in frequency dependence of acoustic properties of canine myocardium. Journal of the Acoustical Society of America, 1989, 86, 2067-2072.	1.1	22

#	Article	IF	CITATIONS
145	Early identification with ultrasonic integrated backscatter of viable but stunned myocardium in dogs. Journal of the American College of Cardiology, 1989, 14, 462-471.	2.8	108
146	Ultrasound integrated backscatter tissue characterization of remote myocardial infarction in human subjects. Journal of the American College of Cardiology, 1989, 13, 84-91.	2.8	111
147	Progress in Quantitative Ultrasonic Characterization of Myocardium: From the Laboratory to the Bedside. Journal of the American Society of Echocardiography, 1988, 1, 294-305.	2.8	61
148	Theoretical Analysis of a Technique for the Characterization of Myocardium Contraction Based Upon Temporal Correlation of Ultrasonic Echoes. IEEE Transactions on Ultrasonics, Ferroelectrics, and Frequency Control, 1987, 34, 368-375.	3.0	30
149	Methods for Estimation of Statistical Properties of Envelopes of Ultrasonic Echoes from Myocardium. IEEE Transactions on Medical Imaging, 1987, 6, 281-291.	8.9	23
150	Ultrasonic Characterization of Canine Myocardium Contraction. IEEE Transactions on Ultrasonics, Ferroelectrics, and Frequency Control, 1986, 33, 347-353.	3.0	30
151	Lateral Resolution in Cardiac Imaging Measured in Vivo. , 1985, , .		1
152	Dependence of tissue characterization features on region of interest (ROI) size: studies on phantoms and simulations. , 0, , .		1